EXPERIMENTAL INVESTIGATION OF PROGRESSIVE DAMAGE AND THE EFFECT OF LAYUP IN NOTCHED TENSILE TESTS

STEPHEN R. HALLETT* AND MICHAEL R.WISNOM

Department of Aerospace Engineering, University of Bristol,

University Walk, BS8 1TR, UK

ABSTRACT: The presence of sub-critical damage in notched composites significantly affects the ultimate failure mode and strength. This paper presents a detailed study of four different layups of E-glass/913 tested using a double-edge-notched specimen loaded in tension. For each layup three different in-plane dimensions are tested. Results are presented in terms of failure mode, strength and sub-critical damage development. Sub-critical damage development is consistent between the layups and between scaled specimens of a single layup. Ultimate failure however shows some variations both with layup and size and this is examined in some detail. The trend of decreasing strength with increasing specimen size is observed for all cases except those where there is a change in failure mode between different size tests. The strengths are compared with predictions from two analytical techniques, which show some ability to achieve correlation across a subset of the test data. Where variations in failure mode occur for a single layup correlation is not possible.

KEYWORDS: notched strength, progressive damage, layup effects, tensile loading

* Author to whom correspondence should be addressed.
E-mail: stephen.hallett@bristol.ac.uk tel:- +44 117 3317098 fax:- + 44 117 927 2771

INTRODUCTION

Any structural material is required to have holes or notches of one sort or another for fasteners, access, weight saving and other reasons. Homogeneous materials exhibit tensile strength reduction due to holes or notches and their associated stress concentrations. Composite materials also show significant sensitivity to notches when loaded in tension, however the effect is less well understood. Whitney and Nuismer[1] introduced the concept of "hole size effect" to describe the reduction in apparent strength with increasingly large holes. Two different size holes although having the same stress concentration will have a different stress gradient in the transverse direction away from the hole. The point and average stress criteria were developed to quantify this effect and how it influences the strength of composites with holes or cracks. This addresses inaccuracies introduced to failure predictions by considering only the hole edge stress by instead considering a characteristic length over the highly stressed area. This parameter needs to be experimentally determined and cannot be applied to different layups once determined from a given test. Other techniques exist for determining the strength of notched composites but since they are largely based on experimentally determined parameters they tend to be specific to one particular lay-up, test configuration or a limited sub-set of the general case. Awerbuch and Madhukar[2] have written an extensive review of such techniques.

Sufficient testing to determine the parameters for use in design calculations is both time consuming and costly. It is therefore desirable to have a predictive model that is accurate across different layups and material systems and requires a minimum number of experimentally measurable material parameters. Any numerical model requires rigorous correlation to physical data. Kortschot and Beaumont[3] have done a detailed study on double-

edge-notched cross-ply specimens investigating damage development prior to ultimate failure, tracking the development of splits in the 0° ply, transverse ply cracks and triangular delamination zones in the 0/90° interfaces. The split and delamination growth was observed to be "self-similar" and a relation between the terminal damage state and specimen strength was found. This indicates a strong influence of the sub-critical damage on the final stress distribution occurring at the notch. Coats and Harris[4] have studied the damage behaviour of a $[\pm 45/0/90/\pm 30/\bar{O}]_s$ layup with different notch sizes for a number of material systems. Results are given for ultimate failure stress and the progressive damage is discussed in qualitative terms from x-ray radiography and de-ply tests. Lagace[5] has investigated the effect of stacking sequence on a range of angle ply laminates with a central hole and found significant effects which are attributed to differences in delamination damage occurring in the hole vicinity. The effect of delamination and interlaminar stresses is significant even in un-notched tensile tests as demonstrated by Sun and Zhou[6].

From the above publications and others it is clear that the sub-critical damage that occurs before complete material failure has a significant effect on the ultimate failure mode and strength. Work by Wisnom and Chang[7] investigated explicitly modelling the individual damage modes occurring within a layup and predicted the sub-critical damage using finite element analysis. This has initially only been applied to cross-ply layups which are commonly used for testing and analysis of notched composites due to their relatively simple stress and damage states [3, 8, 9]. This layup however is not truly representative of those used in typical structural applications e.g. aerospace components, where plies not orthogonal to the loading direction are also included.

The work presented here extends the experimental database, giving detailed results for both progressive and ultimate damage on a range of layups that include ±45º plies. A careful study of the four different layups tested with a double-edge-notched tension specimen has been carried out with a high level of detail for correlation with analytical and numerical models. This data has been used for comparison with finite element analysis which has been developed from techniques first put forward in reference 7 and will be published separately[10]. Although compressive loading has also been shown to cause notch sensitivity[11] this is not considered in this paper.

EXPERIMENTAL SETUP

Hexcel E-glass/913 double-edge-notched specimens (as shown in Figure 1) were tested in tension. Glass/epoxy was used since the material is partially transparent and damage development prior to final failure could be observed in-situ without interrupting the tests. The damage development was monitored from the start of loading and its growth was recorded using a digital video camera. Plates were laid from pre-preg tape and cured according to the manufacturer's instructions in an autoclave giving a nominal ply thickness of 0.125mm. Rectangular specimens were then cut from these plates using a diamond saw. Notches were made at the centre of the specimen using a 100mm diameter, 60° equal angle cutter. Microscopic examination of the notch showed no evidence of damage having been caused during machining. Initially specimens with a total notch length to specimen width ratio (2a/w) of 0.5 and 0.25 were tested. It was found that the 2a/w = 0.5 specimens gave a clearer damage pattern and were therefore selected for use in the programme of testing. Prepared specimens were stored in a desiccating cabinet to remove any effects from ingress of moisture. Tests

were conducted in an Instron universal testing machine at a constant rate of displacement of approximately 1mm/minute.

It is well known that the strength of composite materials varies with the size of specimen tested[12]. One of the aims of this work was to obtain notched strength values for the different layups tested, this could not however be obtained from a single specimen size. The specimen in-plane dimensions for each layup were therefore scaled such that widths of 10, 20 and 40mm were tested. This eliminates the effect of any finite width correction on notched strength and provides a stringent test for analysis, as conventional in-plane finite element modelling would give identical stress fields for the different sized specimens.

Four different layups (shown in Table 1) were tested in the experimental programme. A cross-ply was used as a baseline for comparison to existing work and to produce a relatively simple stress state for analysis. In addition to this, three further layups with ±45º plies were tested. These were a quasi-isotropic layup and two variations, the first with the central load bearing 0º plies removed and the second with two additional plies with 0º plies in the centre.

A typical 20mm wide specimen from each layup tested was de-plied in order to more closely examine the fibre failure and delamination patterns. This was done in a furnace at 500°C for 30 minutes, leaving just enough resin remaining to stop the plies disintegrating. Prior to being placed in the furnace the specimens were soaked in a solution of zinc iodide in 49% water, 49% alcohol and 2% wetting agent to enhance the delamination pattern. When the de-plied specimens were scanned to digital images it was found that this pattern was further enhanced by the penetrant if the fibres were orientated perpendicularly to the scanning direction.

RESULTS

The results from the tests on each of the layups are presented below. Five specimens for each layup were tested for the 10 and 20mm wide specimens and three of each for the 40mm wide specimens. In each case stills from the digital video footage are presented from individual tests that best characterise the general behaviour. The measured far field failure stress for all specimens tested is included in Appendix A.

$[90/0]_s$ Layup

Figure 2 shows a typical load curve for a cross-ply layup. Ultimate failure of the specimen occurs at maximum load. Prior to ultimate failure a split in the 0° fibre direction and a triangular delamination (showing up as a darker region adjacent to the splits) can be observed in Figure 3. The inset shows the early stages of the 0° ply splitting and a single transverse crack in the 90° plies. Percentage of maximum load is shown for each damage state and its position on the load curve is indicated in Figure 2. The 0° fibres fail initially at the notch tip and fracture rapidly progresses across the width of the specimen. The associated load drop can be seen in Figure 2. The fibre failure follows an irregular path across the specimen width and is accompanied by additional splitting and delamination to that seen before the fibre failure. The failure mode was similar across all specimens tested at all sizes.

Figure 4 shows the results obtained from the thermal de-ply of the above specimen. The area of the delamination can be seen as the lighter coloured region and fibre failure has been highlighted with a line for clarity. The top surface of each ply has been shown except for the first ply, which has been turned over to show the delamination on the first interface. Fibre

failure occurs only in the central 0º plies, and as can also be seen in the test photograph this follows an irregular pattern across the width of the specimen.

$[+45/90/-45]_s$ Layup

An examination of the failures of this layup shows a change of failure mode with increasing specimen size (Figure 5). For the 10mm specimens failure is by delamination between the plies with no fibre breakage, which can occur since there are no 0º fibres. In the 20mm wide specimens failure occurs by one of two different modes, either extensive delamination as seen in the 10mm wide specimens or a crack like fracture of broken fibres progressing across the specimen (a sample of each of these modes is shown in Figure 5). The 40mm wide specimens all failed by the second fibre failure dominated mode.

Figure 6 shows the development of sub-critical damage up to the beginning of failure at the maximum load, followed by the final failure mode for a 20mm wide specimen failing in the fibre dominated mode. As with the $[90/0]_s$ specimen damage starts with splits growing in the fibre direction from the notch tip at a relatively low load, although in this case splits are not evident in the 90º ply. Matrix cracks and delamination adjacent to the splits then develop followed by progression of fibre fracture across the specimen width. Thermal deply of the same specimen (Figure 7) shows failure of the central -45º plies at right angles to the loading direction until the fracture has progressed approximately three quarters across the specimen width and then failure is by splitting, delamination and fibre failure of the 90º ply.

$[+45/90/-45/0]_s$ Layup

The quasi-isotropic layup also had some variation in the appearance of the failure both between different size specimens and within a series of tests at the same size. The results are consistent with the $[+45/90/-45]_s$ layup with the smaller specimens having more extensive delamination and the larger specimens cleaner fibre failure with relatively less delamination. Figure 8 shows the progressive failure of one of the 20mm wide specimens. The ultimate failure of the specimen can be seen by the progression of cracks running at 45° from the notch tips. The de-ply results shown in Figure 9 confirm this to be fibre failures in the 0º and 90º plies and splitting in the intermediate -45º ply. The less constrained surface +45º plies failed by splitting and delamination from the adjacent plies in a manner similar to that previously seen in the $[+45/90/-45]_s$ layup.

$[+45/90/-45/0_2]_s$ Layup

Figure 10 shows a graph of applied stress vs. crosshead displacement for a typical $[+45/90/-45/0_2]_s$ layup specimen. It was noted that at the maximum load (point A) only the +45, 90 and -45 degree plies had failed while the central 0° plies remained intact. Figure 11 shows the development of damage in the specimen up to point A. Again the characteristic splitting, delamination and matrix cracking can be seen. However at the maximum load as well as progressive failure across the width of the specimen a large split and delamination area can be seen in the 0º fibre direction. In the final frame of Figure 11 it can be seen that this area of damage extends well away from the notch location and the 0º fibres appear to have locally completely separated from the adjacent plies.

Further extension beyond point A in Figure 10 caused the load to again increase until fibre failure in the 0° plies (point B) and the specimen separated completely. It can be seen in

Figure 12 that the 0° fibre failure is not affected by the position of the notch and is distributed along the length of the specimen between the notch and the testing machine grips. After the load drop at point A the stiffness can be seen to be reducing as fibre damage increases until ultimate failure at point B. The remaining strength at point C can be attributed to a small amount of unbroken fibres and the force required to overcome the friction to pull the interlocking fibres apart.

De-ply of the specimen shown in Figure 11 with the loading stopped after the first load drop (similar to point A, Figure 10) is shown in Figure 13. No fibre failure is visible in the central 0º plies before the adjacent -45º fibres fail. A different specimen was loaded beyond maximum load but interrupted before complete separation of the two halves and then de-plied. In this case distributed failure had started to occur (as could be observed by the partial separation at the notch) however it was not possible to observe the distributed fibre failure in the deplied specimen.

Fibre Fracture Prior To Ultimate Failure

A small number of 20mm wide $[90/0]_s$ and $[+45/90/-45/0]_s$ specimens were loaded to very close to the mean failure load for each layup obtained from the previous series of tests and then interupted. This was done in order to examine the damage prior to ultimate failure. The specimens were then deplied using the method previously described and examined. Figure 14a shows a $[90/0]_s$ specimen before loading and Figure 14b shows the same specimen loaded to 91% of the mean failure load. Figure 14c and d show microscope views of the deplied 0° fibres at the notch tip. Fibre breaks can be seen starting at the notch tip in a crack like pattern. Figure 14e to h shows results of a similar test for a $[+45/90/-45/0]_s$ specimen loaded to 97% of mean failure load. In other tests, almost identical to those shown, no evidence of fibre failure was observed. This is thought to be due to the statistical variation in specimen strength. In

those tests where no fibre failure was observed the strength was assumed to be somewhat above the mean and therefore the load at which the test was interrupted was not sufficient to initiate fibre failure. This seems to indicate that while a very small amount of stable crack like growth occurs in the 0° plies of a laminate, it only occurs very close to the ultimate failure load.

Transverse cracking

In addition to the splitting and delamination damage that occurs in the specimens, transverse cracking can be seen to develop with the crack density increasing with applied load. This is most clearly seen in the cross-ply ($[90/0]_s$). The average matrix crack spacing in a 20mm wide crossply specimen was measured just prior to failure. This was found to be 0.3mm and distributed evenly between the splits as can be seen in Figure 15.

Figure 16 shows the stress-displacement curve as measured from a typical test. A non-contacting video extensometer as described by Towse et al [13] and markers on the specimen either side of the notches seen in Figure 15 were used to obtain an accurate measurement of displacement across the notch as opposed to cross-head displacement. Also shown on Figure 16 is a measure of the specimen stiffness using the gradient as it changes over the period of loading. After an initial bedding in of the specimen and before ultimate failure a stiffness loss of approximately 50% is observed. Much of this can be attributed to the geometry of the specimen and the growth of the splits with increasing load.

The presence of the matrix cracking will also affect the material stiffness. An analysis developed by Kashtalyan and Soutis[14] predicts the reduction in laminate stiffness with

increasing transverse crack density. For a $[90/0]_s$ E-glass epoxy cross-ply laminate with 30 cracks/cm this predicts an 15% reduction in axial stiffness.

A similar crack density was observed for the 10mm wide crossply specimens but a reduced crack spacing of 0.6mm was observed for the 40mm wide specimens.

Size effect

Strength

In order to quantify the effect of increasing specimen size, the maximum stress for the different layups was plotted against specimen width in Figure 17 using the far field applied stress calculated from force divided by gross cross section area. Only the mean value from each data set has been plotted together with the standard deviation. The straight lines plotted in Figure 17 are for visualisation only and are not fitted curves. The trend of reducing strength with increasing specimen size is similar for all layups with the one noticeable exception being the 10 to 20mm wide specimens for the $[45/90/-45]_s$ lay-up where similar strengths were obtained. This is due to the change in failure mode from delamination and pullout of the plies to fibre failure. Only the in-plane specimen dimensions are scaled, therefore the cross section area over which applied stress is acting has doubled while the area of delamination required to cause failure by pullout of the plies has quadrupled. The applied stress required to cause delamination failure by pull-out of the plies therefore increases to above that required to cause fibre failure as the specimen size increases. For the 20mm wide specimens these stresses must be approximately equal as failure can occur by either mode.

Converting the stresses shown in Figure 17 to strains using an effective modulus for each layup gives results shown in Figure 18. It can be seen that the two layups in which the

maximum stress is controlled by 0° fibre failure ($[90/0]_s$ and $[45/90/-45/0]_s$) have very similar failure strain. The remaining two layups ($[45/90/-45]_s$ and $[45/90/-45/0_2]_s$) do not show any consistent trends between them due to the variation in failure modes.

Damage Mode

It has already been noted that there are some differences in the failure modes at different sizes for the layups considered. Those layups that show no change in damage mode are also worth closer observation. The cross-ply layup has almost identical failure patterns for all sizes as can be seen in Figure 19. In all cases the fibre damage has progressed across the specimen in a crack-like manner that is accompanied by a band of splitting and delamination. The extent of the damage zone does not scale with specimen size but is approximately constant. Floyd et al[15] have employed an approach based on this effect to include size effect in their numerical modelling of single notched specimens. Determining suitable values for use in the analysis is in practice difficult, particularly for the more complex layups as can be seen by Figure 20 , which shows results for typical quasi-isotropic specimens.

Split Growth

The length of the split in the 0º ply has been recorded for all three specimen sizes for the $[90/0]_s$ and $[45/90/-45/0]_s$ layups. In each case the first three specimens for each size were measured since for the largest specimen size this was the total number of specimens tested. The $[45/90/-45]_s$ and $[45/90/-45/0_2]_s$ layups were excluded from this study due to the variation in failure modes. This measurement was taken from the digital video footage with the length (L) defined as the distance from the notch tip to the split end and recorded as the average of the four splits occurring in each specimen.

Figure 21a shows the increase in split length with increasing specimen size with respect to applied stress. Whilst the split growth rate increases with specimen size the stress at which it initiates remains approximately constant at 60MPa. Figure 21b shows the split length (L) normalised by the notch size (a) with respect to applied stress. The data for the 10 and 20mm wide specimens now converges to a single curve. The largest specimen size at the longest split lengths shows a slight deviation from this curve at larger split lengths. This may well be due to interaction between different sub-critical damage modes e.g. distributed fibre failure which is defect controlled and therefore more likely to occur in the larger volume of material. Figure 21c shows the delamination area associated with a single split length L, again averaged over the four delamination areas in each specimen. Figure 21d shows the delamination area versus split length squared. This is approximately linear and thus indicates that the delamination growth is "self-similar" and its relation to the split growth is not size dependant.

Figure 22 shows the split growth data for the $[45/90/-45/0]_s$ specimens. Firstly the split in the 0° ply only has been measured and presented as a mean of the four 0° split lengths (L) in Figure 22a and then normalised by the notch width (a) in Figure 22b. In Figure 22c and d the same presentation has been made for the total length of the splits in the 0°, +45° and -45° plies averaged over the number of splits measured. The 90° split was not of sufficient length or prominence to be measurable. As with the $[90/0]_s$ layup an increase in split length with increasing specimen size was observed for both the split in the 0° plies and the total split length. When normalised by the notch width the data does come together to form an approximately straight line master curve but the scatter is significantly greater than for the $[90/0]_s$ layup and in the case of the total split length it can be noticed that there is a slight

decrease in relative split length with increasing specimen size. The delamination area could not easily be measured as was done in the case of the $[90/0]_s$ layup.

DATA ANALYSIS

In this section the data produced by the tests is compared with two published analysis techniques for predicting notched failure.

Probably the best known analysis of notched composite data is that performed by Whitney and Nuismer [1] who developed the concept of point and average stress criteria. Using equation 1 as developed in [16] for a centre cracked specimen, the average stress criterion has been applied to the mean results for the $[90/0]_s$ and $[+45/90/-45/0]_s$ layups. The other two layups tested have not been analysed due to the changes in failure mode between specimen size and the distributed failure not located at the notch.

$$\frac{\sigma_N^{\infty}}{\sigma_0} = \sqrt{\frac{1 - \frac{c}{(c+a_0)}}{1 + \frac{c}{(c+a_0)}}} \qquad \text{Equation (1)}$$

where σ^{∞}_N is the infinite width notched strength, σ_0 is the un-notched strength, c is the half crack length and a_0 is the distance over which the average stress is taken. An isotropic finite width correction factor (Y) for a centre cracked specimen[2] (equation 2) has been used. It is reported that the error associated with not using an orthotropic finite width correction factor is not significant[2].

$$\mathbf{Y} = 1 + 0.1282\left(\frac{\mathbf{2a}}{\mathbf{W}}\right) - 0.2881\left(\frac{\mathbf{2a}}{\mathbf{W}}\right)^2 + 1.5254\left(\frac{\mathbf{2a}}{\mathbf{W}}\right)^3 \qquad \text{Equation (2)}$$

The un-notched strength has been calculated using 3.48% strain to failure (the mean value from three sets of experiments performed by Wisnom and Atkinson[17]) and the effective modulus. An average stress distance (a_0) of 1.19mm in equation 1 gave the best fit to the $[90/0]_s$ experimental data points using the least squares method. Equation 1 (with a_o=1.19mm) is plotted along with mean test values in Figure 23. This same value of a_0 in equation 1 did not give good agreement to the failure stresses for the $[+45/90/-45/0]_s$ layup where a value of 2.37mm was required to obtain a good fit to the test data (also shown in Figure 23).

Vaidya and Sun[18] have developed a fracture criterion from experimental results on AS4/3501-6 based on fracture toughness and the stresses in the 0º ply which are assumed to govern failure. This analysis requires a constant value for the laminate fracture toughness (K_Q) to be established for each layup from which an approximately constant 0º ply fracture toughness (K^0_Q) for all layups can be established. Equation 3 has been used for the calculation of the fracture toughness for each layup from the present data.

$$K_Q = Y\sigma_f\sqrt{\pi a} \qquad \text{Equation (3)}$$

Where Y is the finite width correction factor (calculated using equation 2), a is the half crack length and σ_f is the remote applied stress at failure. The mean result from each specimen size in the current investigation is shown in Figure 24 for the $[90/0]_s$ and $[+45/90/-45/0]_s$ layups. Values for the $[+45/90/-45]_s$ and $[+45/90/-45/0_2]_s$ layups have not been calculated for such an analysis since in these cases as discussed previously failure is not governed by failure of 0º

plies. The lines joining the data points are straight lines for visualisation only. The values do collapse down to a single curve for K^0_Q if multiplied by the stress ratio η (stress in 0° plies divided by σ_f) but it can be seen that a constant value is not obtained as for data in reference 18 although the trend is towards an asymptote at larger values of a.

DISCUSSION

Under quasi-static tensile loading damage initiates in the specimen at a relatively low load compared to the ultimate failure stress. In the case of the cross-ply laminate this damage separates into direct and shear driven behaviour. The former is shown by cracks in between fibres or fibre tows within the 90° plies of the laminate, evenly distributed in the region between the notches. The latter takes the form of splits in the 0° plies starting from the notch tip and increasing in length with applied load. For the laminates containing 45° plies a similar behaviour is observed but the distinction between the shear and direct loading causing distinct damage modes is no longer clear. Splits grow within the plies starting from the notch tips and are accompanied by cracks distributed throughout the highly loaded region between the notches.

The distinction between the term “crack” and “split” is best made by their location and the nature of their growth. “Splits” initiate at the notch tip only and their growth is characterised by an increase in length and is accompanied by an area of delamination adjacent to the split. “Cracks” are distributed through out the highly loaded region and their distribution is approximately evenly spaced. Their growth is characterised by an increase in the area affected and crack density. They are not generally accompanied by delamination in tests performed

here but have been reported to be the site of initiation of delamination[19] in the case of tensile loaded un-notched carbon fibre. The difference in observed growth between "cracks" and "splits" is largely due to the constraint conditions imposed by their location, being either within the material in the case of "cracks" or starting at a free edge in the case of "splits".

With regard to the ultimate failure of the specimens there are again two different modes of failure that are dependent on constraint conditions of the material although in this case they are caused by different mechanisms. The clearest example of this is the $[+45/90/-45]_s$ layup which has the potential to fail by delamination alone without any fibre failure, with the plies simply sliding out from between each other. This occurs in the case of the smaller 10mm wide specimens, however none of the 40mm wide specimens failed in this mode, failing instead by crack-like fibre failure progressing across the width of the specimen. There appears therefore to be insufficient energy to cause interlaminar failure, due to the increased delamination area that would be required and fibre failure instead occurs first. The 20mm wide specimens show some variation between these two failure modes, thus indicating a statistical variation in the material strengths.

The investigations have attempted to determine the nature of the fibre failure through thermal deply of failed specimens. There is evidence from the literature of both a distributed statistical failure of individual fibres or fibre bundles which eventually lead to ultimate failure of a specimen[20,21] and of crack-like failure progressing across a specimen initiating from a stress concentration[22]. Results from tests presented here have elements that support both hypotheses. The stiffness loss of the cross ply laminate with increasing load cannot be attributed to matrix cracking alone, even after the specimen geometry, splitting and delamination have been taken into account. This suggests that there is some accumulating damage to the load bearing 0°

plies. The $[-45/90/45/0_2]_s$ layup gives further evidence of the presence of distributed fibre breaks in that once the effect of the stress concentration due to the notch is removed, stiffness reduction continues and ultimate failure results in the brush like appearance shown in Figure 12. In the other layups the effect of the stress concentration appears to be sufficient to initiate failure at the notch tip and once initiated it progresses across the specimen. A microscopic analysis of the notch tip prior to ultimate failure showed the presence of a number of broken fibres, thus indicating the site of failure initiation. This only occurred at loads very close to ultimate failure and was therefore difficult to repeat due to the statistical variation in specimen strength.

Three different size specimens were tested for each layup in order to better understand the effect of size on the results produced. Only the in-plane dimensions were scaled with the ratio of notch to specimen width kept constant to avoid any variation in finite width correction factor. A significant observation from the scaled tests was the variation in failure mode with specimen size and layup. A reduction in strength with increasing size was found in the majority of cases. A more detailed study of the effect of size is being carried out under a different programme of work.

The strength results from the different layups and specimen sizes have been compared to two different analytical techniques for predicting the notched behaviour. Both show areas of applicability to a sub-set of the results but they do not completely capture the effect of notch size across the different layups tested. It is acknowledged that there are numerous other analytical techniques available, many of which are variations on those presented here. An approach that has been adopted by the authors is to predict the sub-critical damage that has been observed in the tests presented here using finite element analysis. These models have

then been used to investigate the effect of this damage on the notched strength of different layups and specimen sizes[10].

CONCLUSION

In conclusion it can be seen that the failures due to notches in composite materials are complex and vary both with layup and specimen size. Not only do the failure stresses vary but also significant variation in the failure modes is observed. It has not been possible to completely characterise the failure stresses using the analytical techniques applied here based on either fracture mechanics or the average stress criterion. Further development of more complex models which take account of the different damage modes and sub-critical damage are therefore required before accurate predictions can confidently made across a range of sizes, layups and materials.

The detail of the test results presented here shows evidence of the different failure modes occurring in the specimens and provides a significant body of data for correlation of analytical and numerical models for prediction of failure.

LIST OF FIGURES

TABLES

$[90/0]_s$
$[+45/90/-45]_s$
$[+45/90/-45/0]_s$
$[+45/90/-45/0_2]_s$

Table 1 Lay-ups tested

APPENDIX A: FAILURE STRESSES FOR ALL SPECIMENS TESTED

Test No.	$[90/0]_s$ Max Stress (MPa)			$[45/90/-45]_s$ Max Stress (MPa)		
Specimen width	**10mm**	**20mm**	**40mm**	**10mm**	**20mm**	**40mm**
1	311.0	291.0	204.2	158.8	148.3	135.9
2	320.8	263.7	237.5	162.4	159.3	130.2
3	280.2	254.6	237.5	162.4	174.0	135.0
4	292.4	280.8		154.3	171.7	
5	326.2	243.4		165.1	168.9	
Mean	**306.1**	**266.7**	**226.4**	**160.6**	**164.5**	**133.7**
Std Dev	19.4	19.3	19.2	4.2	10.6	3.1
CV (%)	6.3	7.2	8.5	2.6	6.5	2.3

Test No.	$[45/90/-45/0]_s$ Max Stress (MPa)			$[45/90/-45/0_2]_s$ Max Stress (MPa)		
Specimen width	**10mm**	**20mm**	**40mm**	**10mm**	**20mm**	**40mm**
1	221.2	211.3	163.0	346.3	317.2	296.0
2	203.9	213.6	180.4	328.3	300.8	293.5
3	238.0	195.8	169.7	331.0	327.2	282.5
4	226.8	201.3		336.3	315.0	
5	222.2	203.4		311.1	324.5	
Mean	**222.4**	**204.3**	**171.0**	**330.6**	**316.9**	**290.6**
Std Dev	12.3	6.1	8.8	12.9	10.3	7.2
CV (%)	5.5	3.0	5.1	3.9	3.3	2.5

REFERENCES

1 Whitney, J.M. and Nuismer, R.J. (1974). Stress fracture criteria for laminated composites containing stress concentrations, *Journal of Composite Materials*, **8**: 253-265

2 Awerbuch, J. and Madhukar, M.S. (1985). Notched strength of composite laminates: Predictions and experiments - A review, *Journal of Reinforced Plastics and Composites*, **4**: 3-159

3 Kortschot, M.T. and Beaumont, P.W.R. (1990). Damage mechanics of composite materials I: Measurements of damage strength, *Composites Science and Technology*, **39**(4): 289-301

4 Coats, T.W. and Harris, C.E. (1999). A progressive damage methodology for residual strength predictions of notched composite panels, *Journal of Composite Materials*, **33**(23): 2193-2232

5 Lagace, P.A. (1986). Notch sensitivity and stacking sequence of laminated composites, *Composite Materials: Testing and Design (Seventh Conference), ASTM STP 893*, 161-176

6 Sun, C.T. and Zhou, S.G. (1988). Failure of quasi-isotropic composite laminates with free edges, *Journal of Reinforced Plastics and Composites*, **7**: 515-557

7 Wisnom, M.R. and Chang, F.K. (2000). Modelling of splitting and delamination in notched cross-ply laminates, *Composites Science and Technology*, **60**(15): 2849-2856

8 Liu, C.J., Sterk, J.C., Nijhof, A.H.J. and Marissen, R. (2002). Matrix-dominated damage in notched cross-ply composite laminates: experimental observations, *Applied Composite Materials*, **9**: 155-168

9 Aymerich, F., Mannu, M. and Priolo, P. (2002). Damage mechanisms in notched graphite/epoxy laminates, *Proceedings of American Society for Composites*, 17th Annual Technical Conference, West Lafayette

10 Hallett, S.R. and Wisnom, M.R. (to be published). Numerical investigation of progressive damage and the effect of layup in notched tensile tests

11 Soutis, C. (1994). Damage tolerance of open-hole CFRP laminates loaded in compression, *Composites Engineering*, **4**(3): 317-327

12 Wisnom, M.R. (1999). Size effects in the testing of fibre-composite materials, *Composites Science and Technology*, **59**(13): 1937-1957

13 Towse, A., Setchell, C., Potter, K.D., Clarke, A.B., Macdonald, J.H.G., Wisnom, M.R. and Adams, R.D. (2001). Use experience with a developmental general purpose non-contacting extensometer with high resolution, *Nontraditional Methods of Sensing Stress, Strain, and Damage in Materials and Structures, ASTM STP 1323*: 36-51

14 Kashtalyan, M. and Soutis, C. (2000). Stiffness degradation in cross-ply laminates damaged by transverse cracking and splitting, *Composites: Part A*, **31**(4): 335-351

15 Floyd, A., Vaziri, R. and Poursartip, A. (2003). Modelling Specimen Size Effect in Laminated Composites, *Proceedings of the 14th International Conference on Composite materials (ICCM14), San Diego*

16 Nuismer, R.J. and Whitney, J.M. (1975). Uniaxial failure of composite laminates containing stress concentrations, *Fracture Mechanics of Composites, ASTM STP 593*, 117-142

17 Wisnom, M.R. and Atkinson, J.W. (1997). Reduction in tensile and flexural strength of unidirectional glass fibre-epoxy with increasing specimen size, *Composite Structures*, **38**(1-4): 405-411

18 Vaidya, R.S. and Sun, C.T. (1997). Fracture criterion for notched thin composite laminates, *AIAA Journal*, **35**(2): 311-316

19 Takeda, N. and Ogihara, S. (1994). Initiation and growth of delamination from the tips of transverse cracks in CFRP cross-ply laminates, *Composites Science and Technology*, **52**(3): 309-318

20 Okabe, T. and Takeda, N. (2002). Size effect on tensile strength of unidirectional CFRP compites - experiment and simulation, *Composites Science and Technology*, **62**(16): 2053-2064

21 Wisnom, M.R. (2000). Modelling progressive fibre failure with size effect, *Proceedings of American Society for Composites*, 15th Annual Technical Conference, Texas: 639-648

22 Kongshavn, I. and Poursartip, A. (1999). Experimental investigation of a strain-softening approach to predicting failure in notched fibre-reinforced composite laminates, *Composites Science and Technology*, **59**(1): 29-40

FIGURES

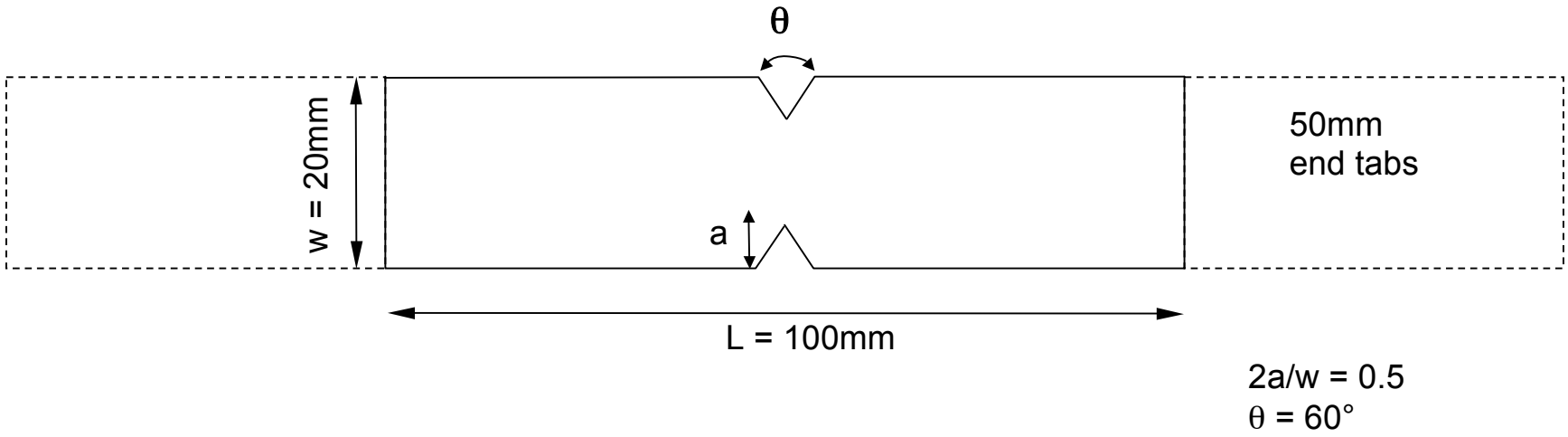

Figure 1 Specimen geometry for 20mm wide specimen

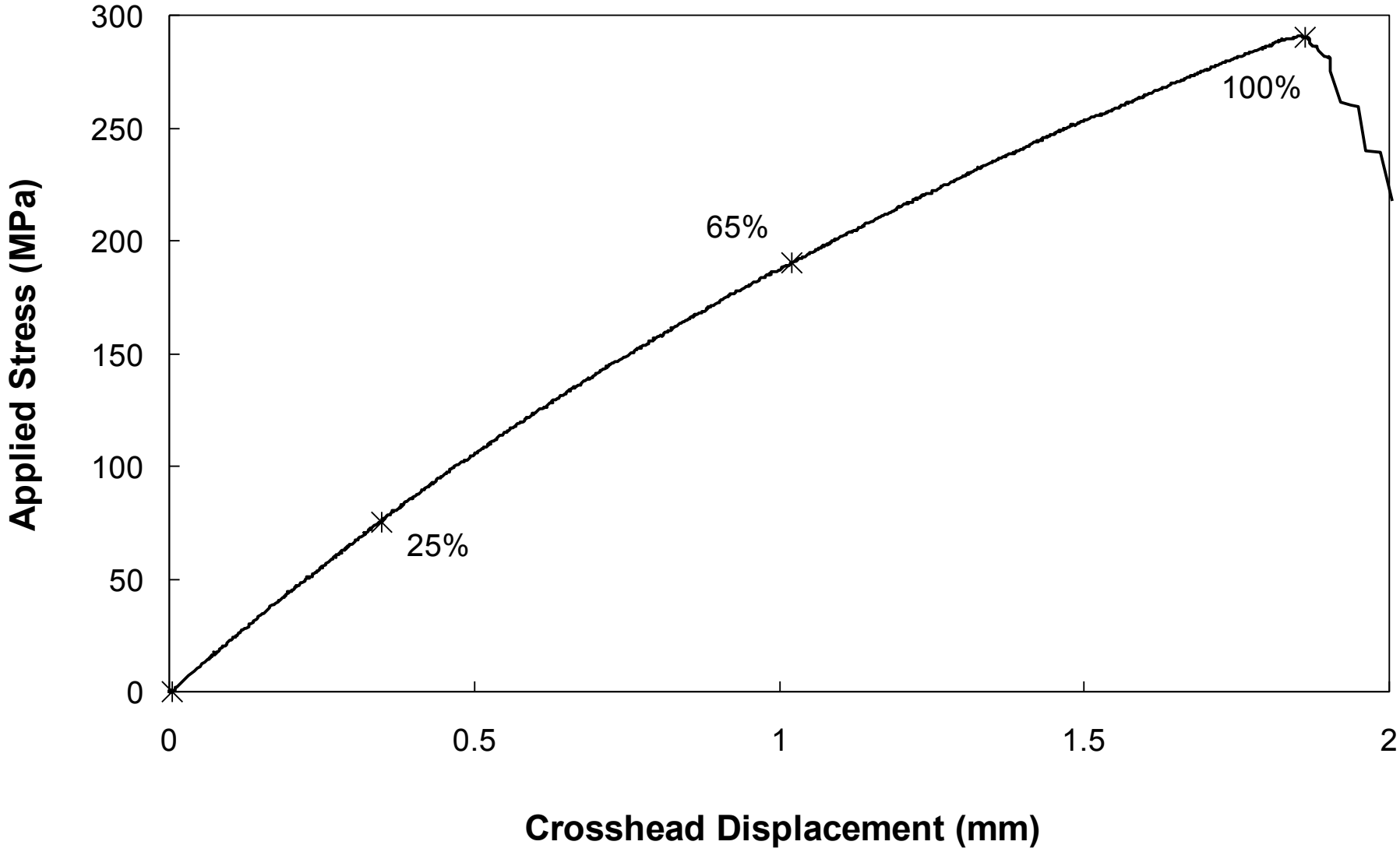

Figure 2 Stress-Displacement graph for a typical $[90/0]_s$ specimen

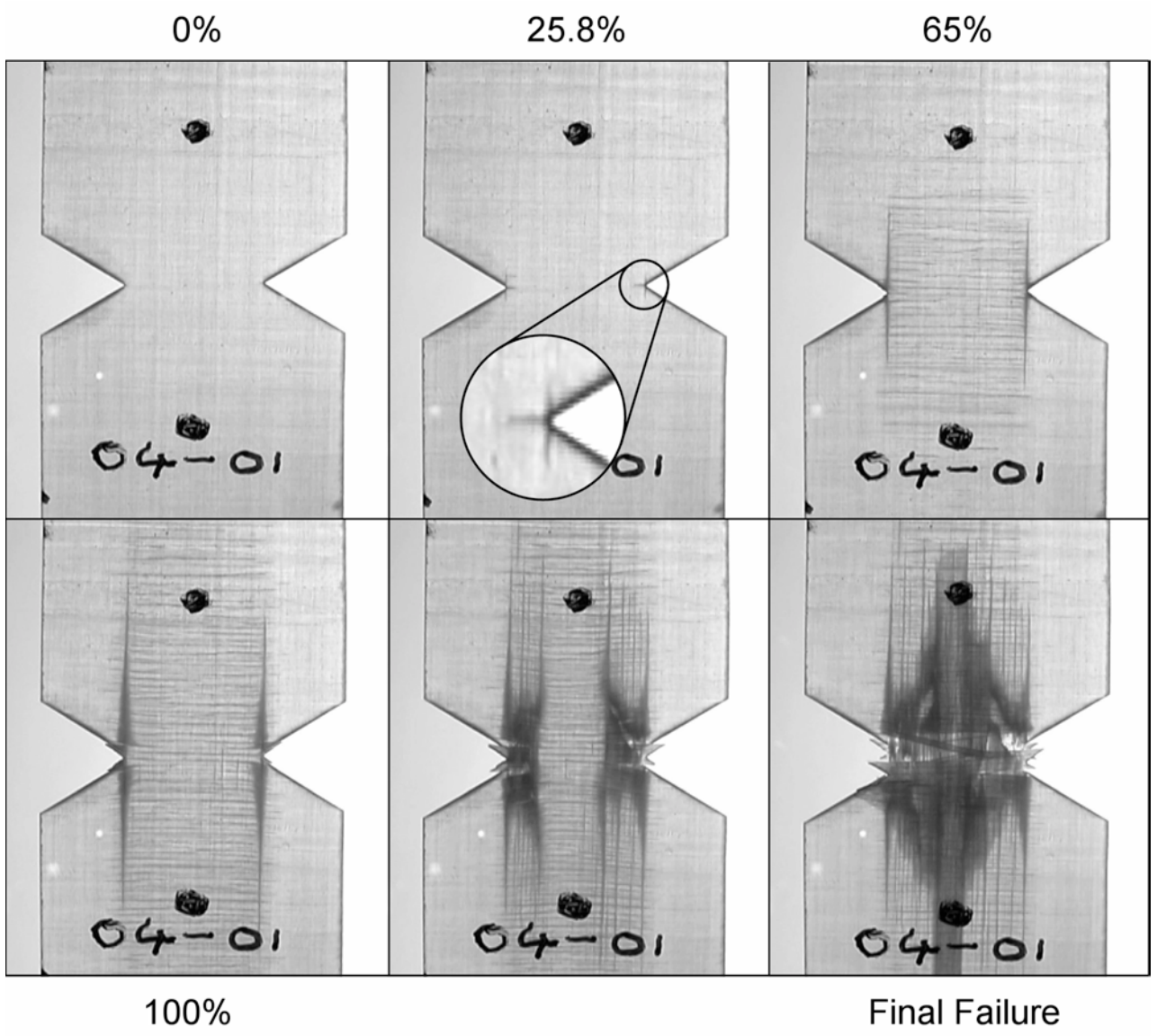

Figure 3 Progressive failure of a 20mm wide $[90/0]_s$ specimen (% maximum load shown)

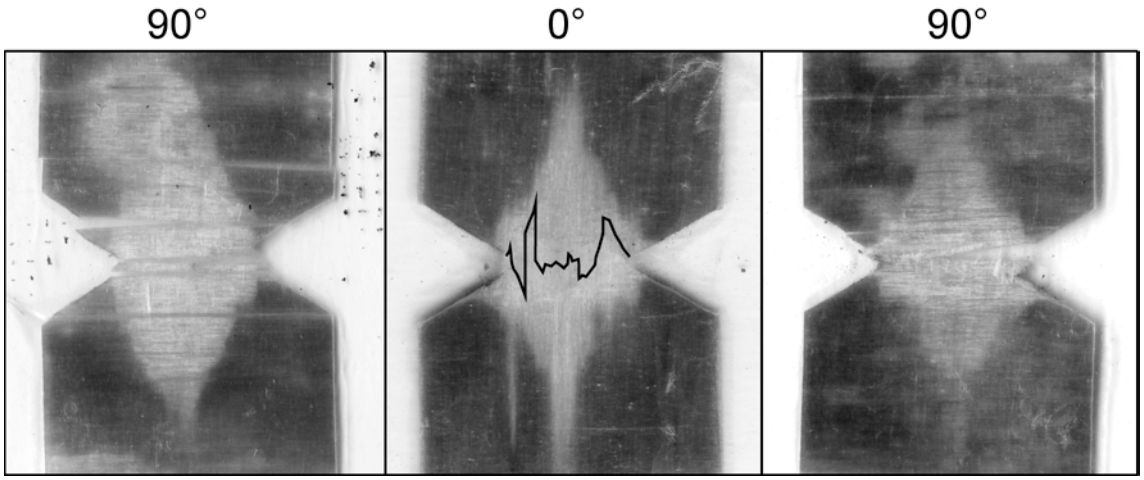

Figure 4 Deplied $[90/0]_s$ specimen showing delamination and fibre failure

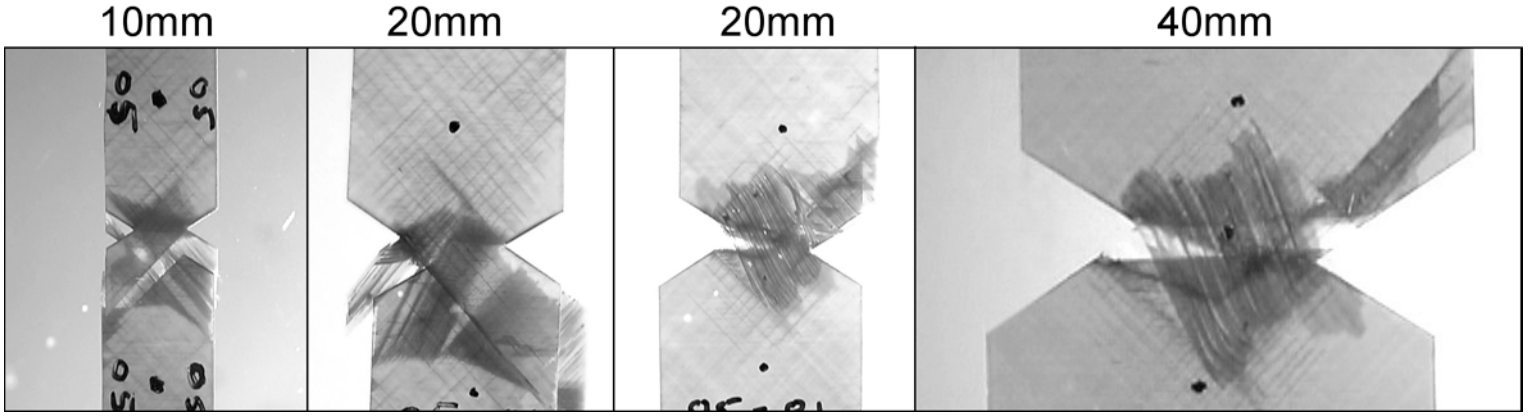

Figure 5 Failure modes of the $[+45/90/-45]_s$ specimens tested

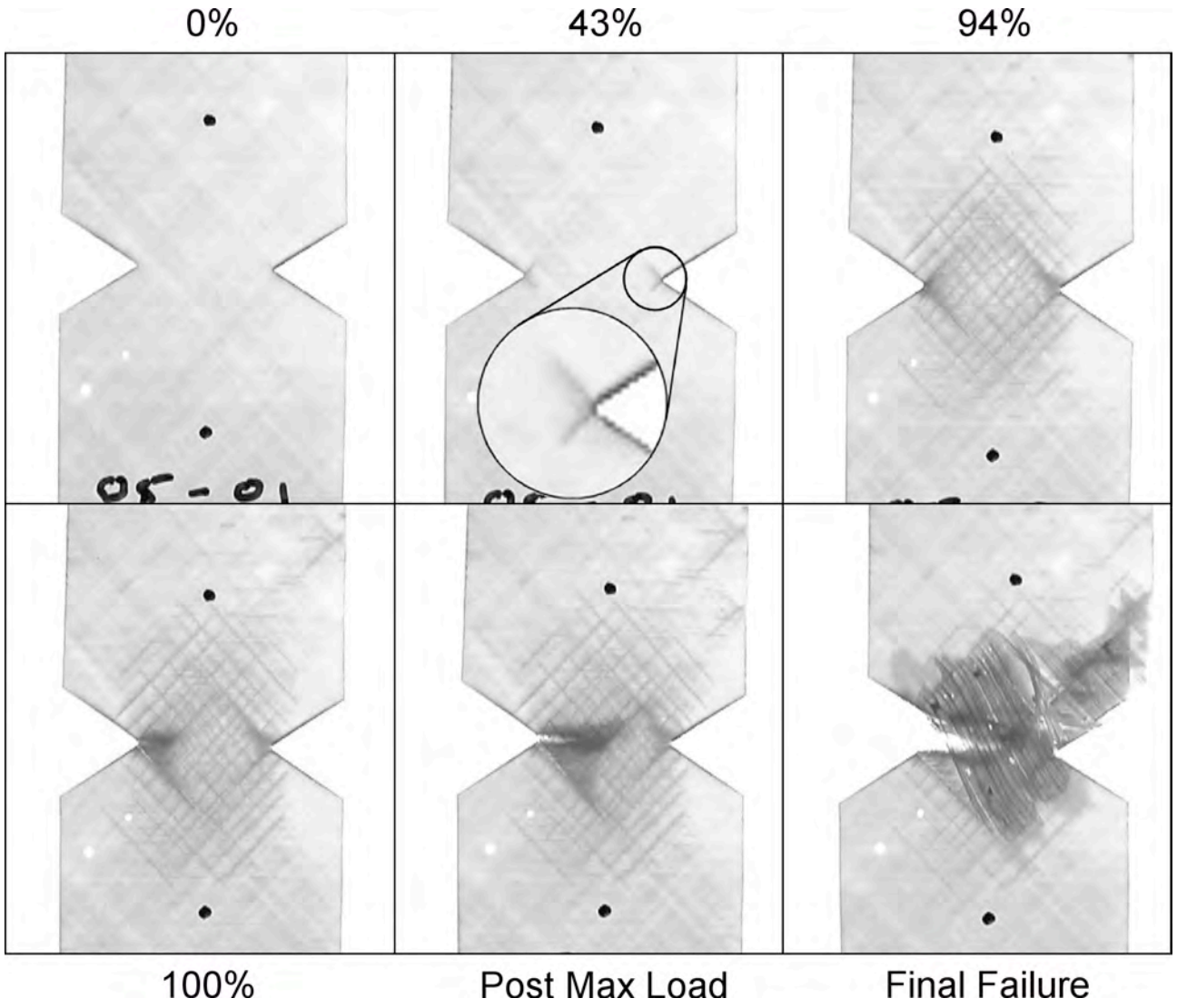

Figure 6 Progressive failure of a 20mm wide $[45/90/-45]_s$ specimen (% maximum load shown)

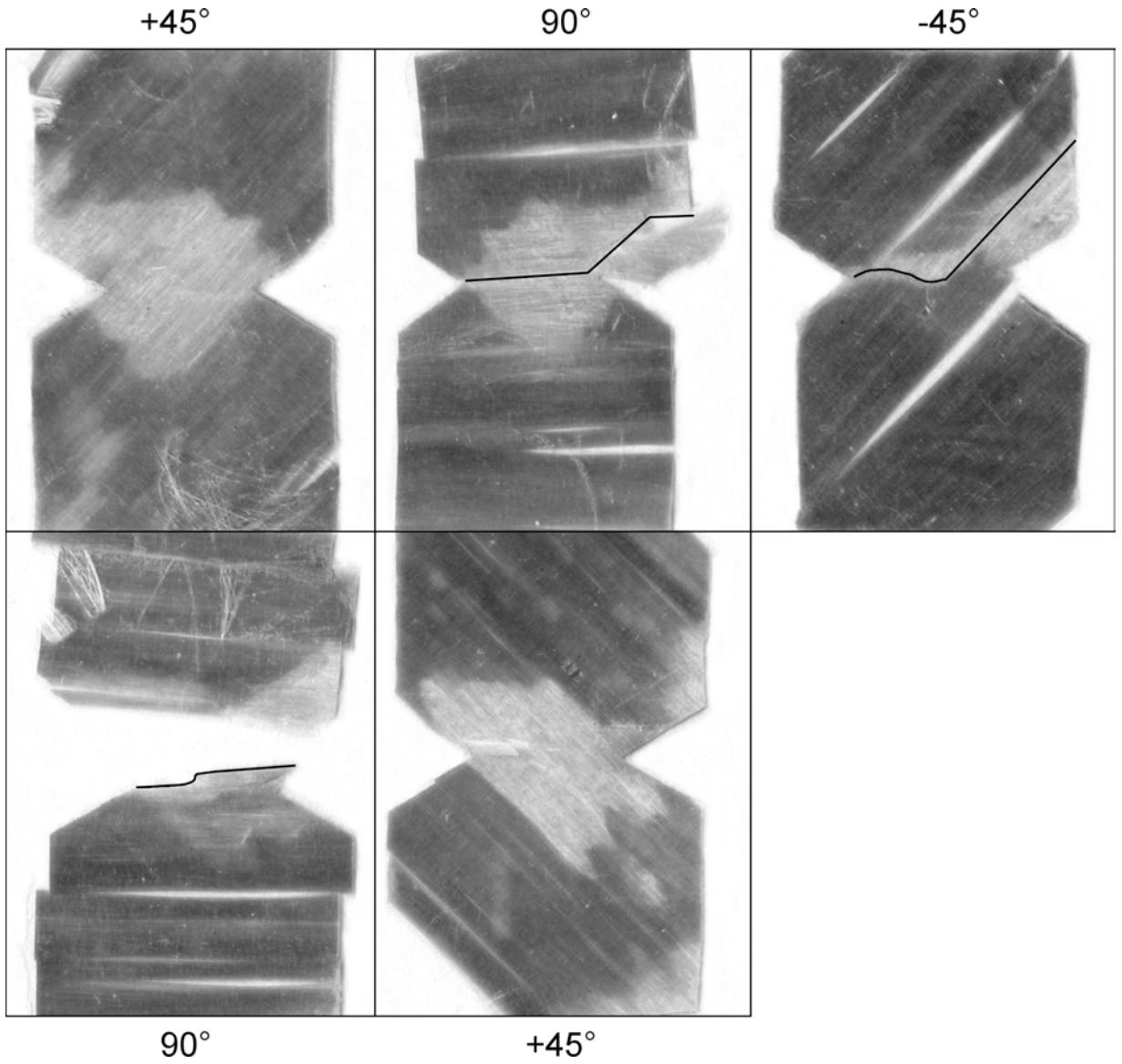

Figure 7 Deply of the $[+45/90/-45]_s$ specimen shown in Figure 6 showing delamination and fibre failure location

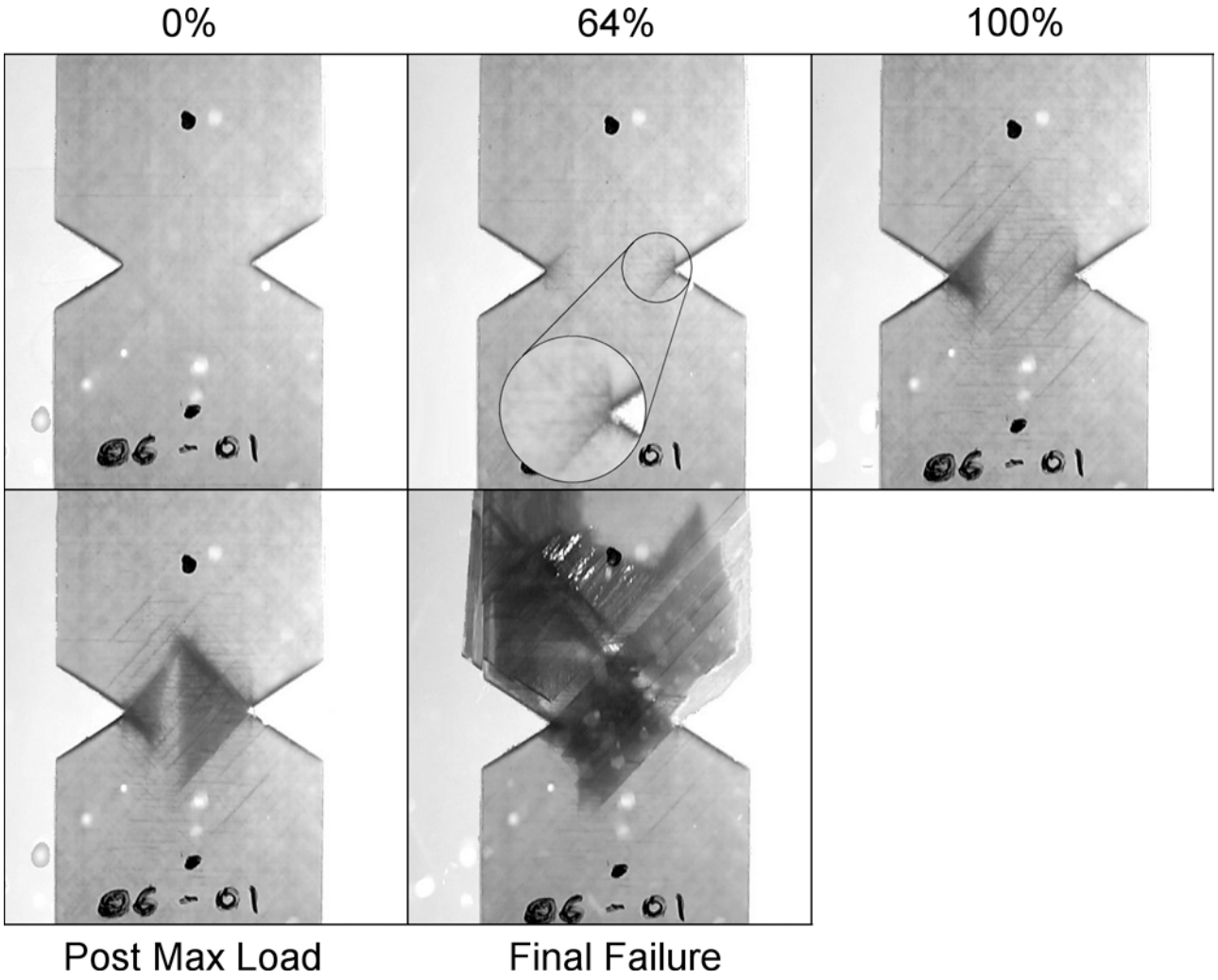

Figure 8 Progressive failure of a 20mm wide $[45/90/-45/0]_s$ specimen (% maximum load shown)

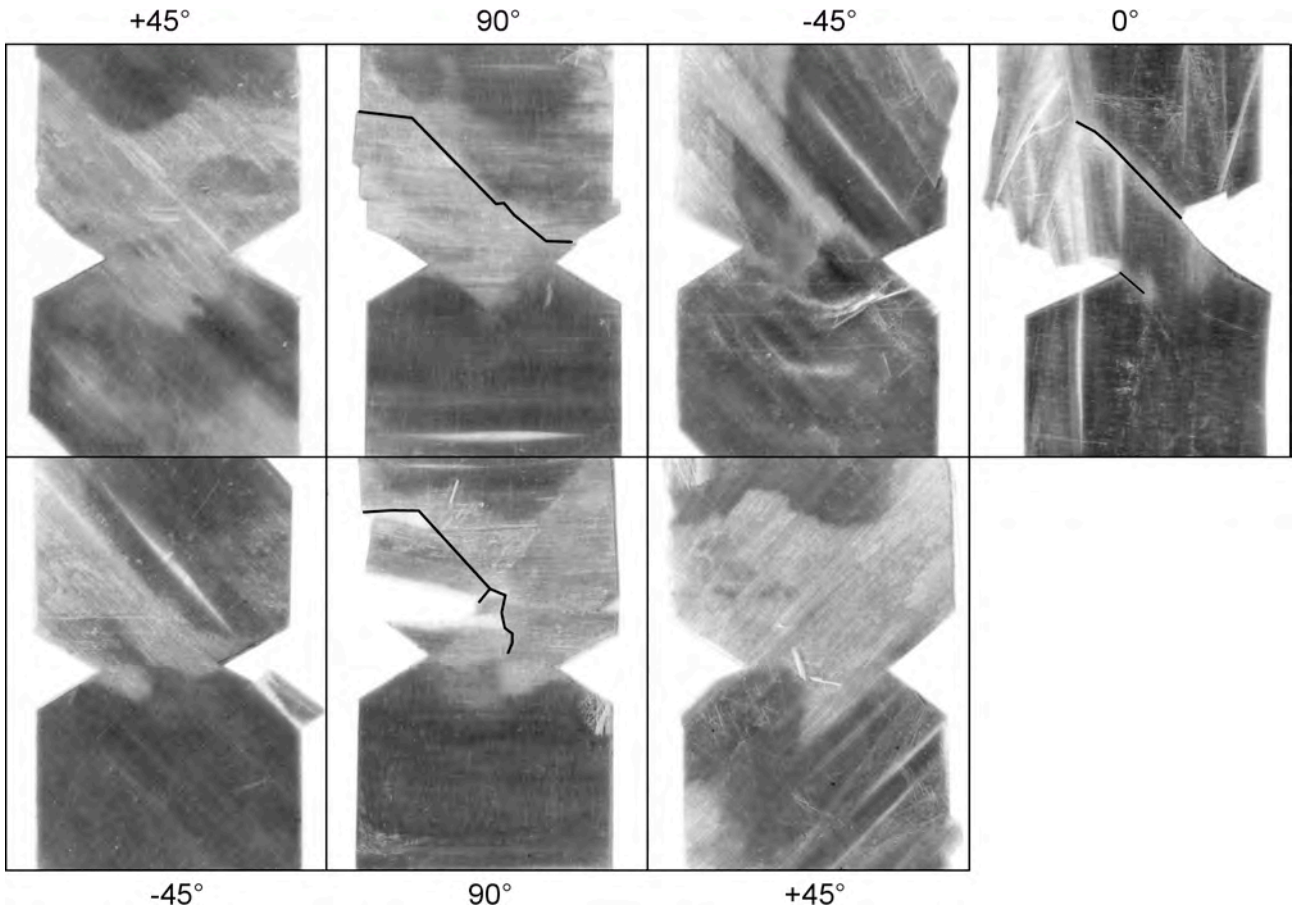

Figure 9 Deply of the $[+45/90/-45/0]_s$ specimen shown in Figure 8 showing delamination and fibre failure location

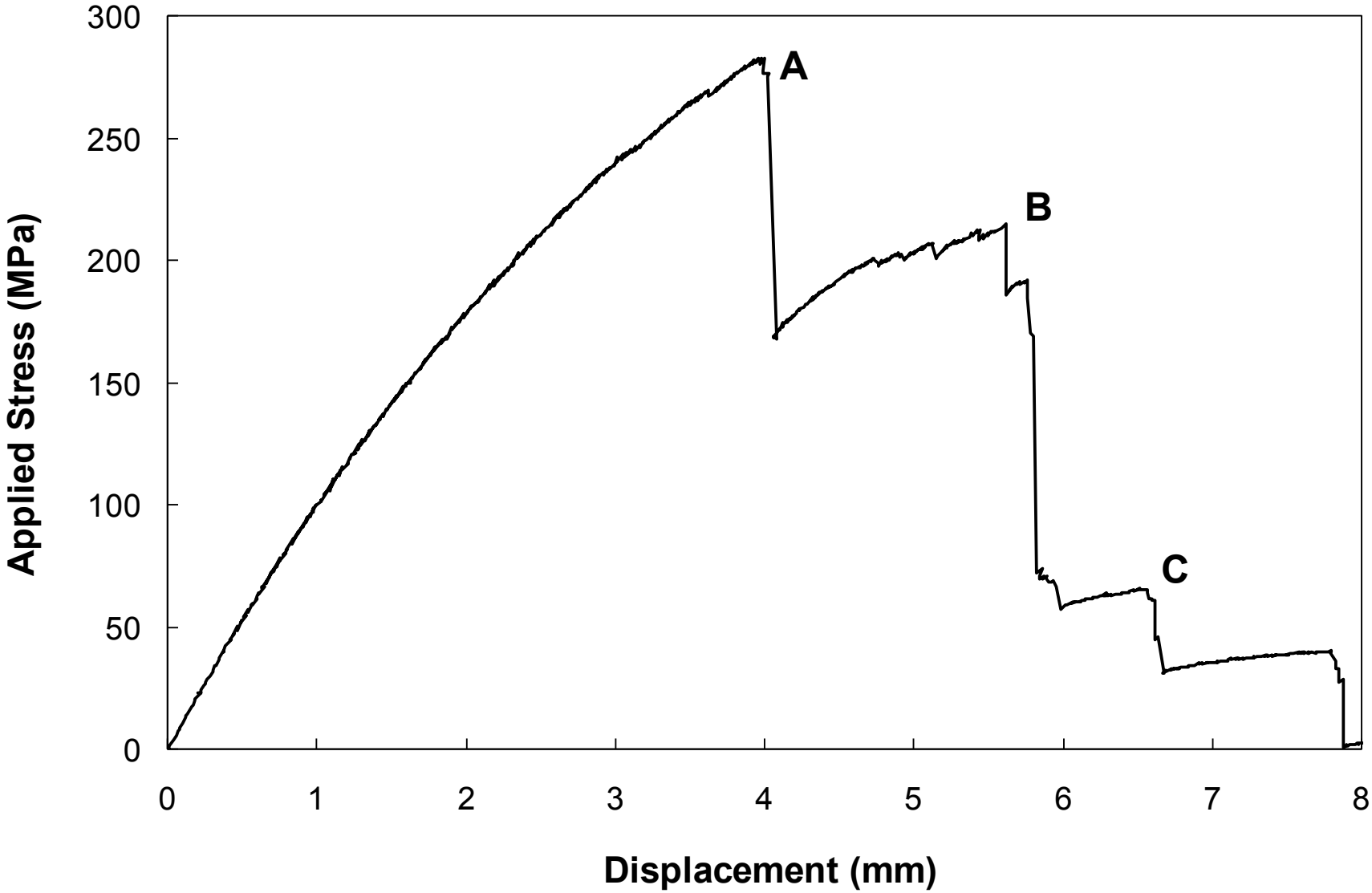

Figure 10 Applied stress vs. crosshead displacement graph for a typical $[+45/90/-45/0_2]_s$ specimen

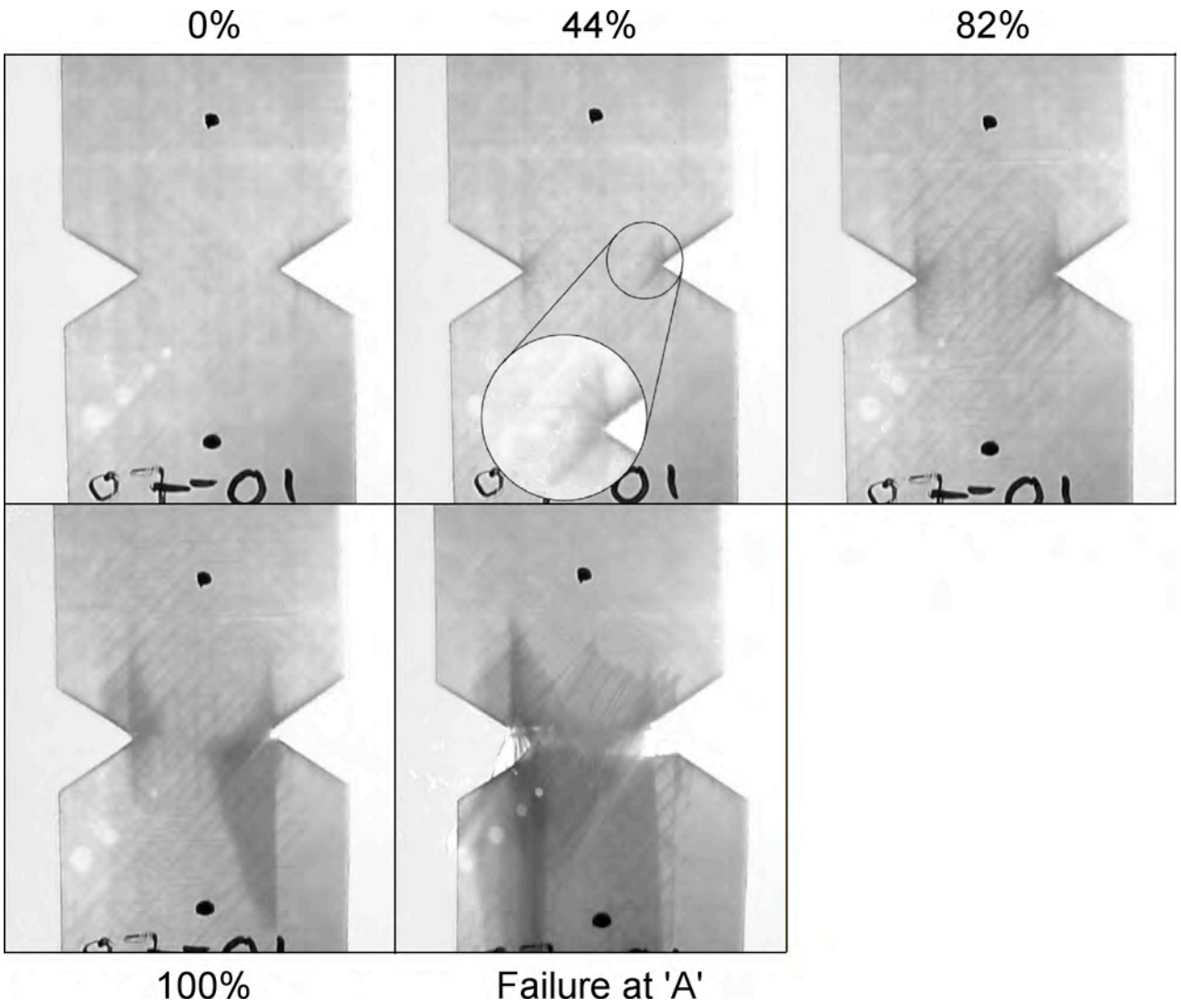

Figure 11 Progressive failure of a 20mm wide $[45/90/-45/0_2]_s$ specimen (% maximum load shown)

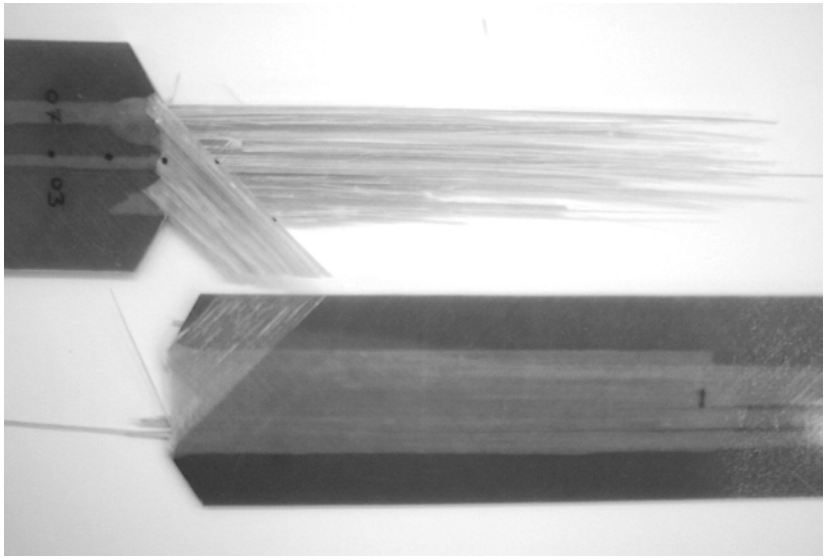

Figure 12 Ultimate failure pattern of a 40mm wide $[+45/90/-45/0_2]_s$ specimen

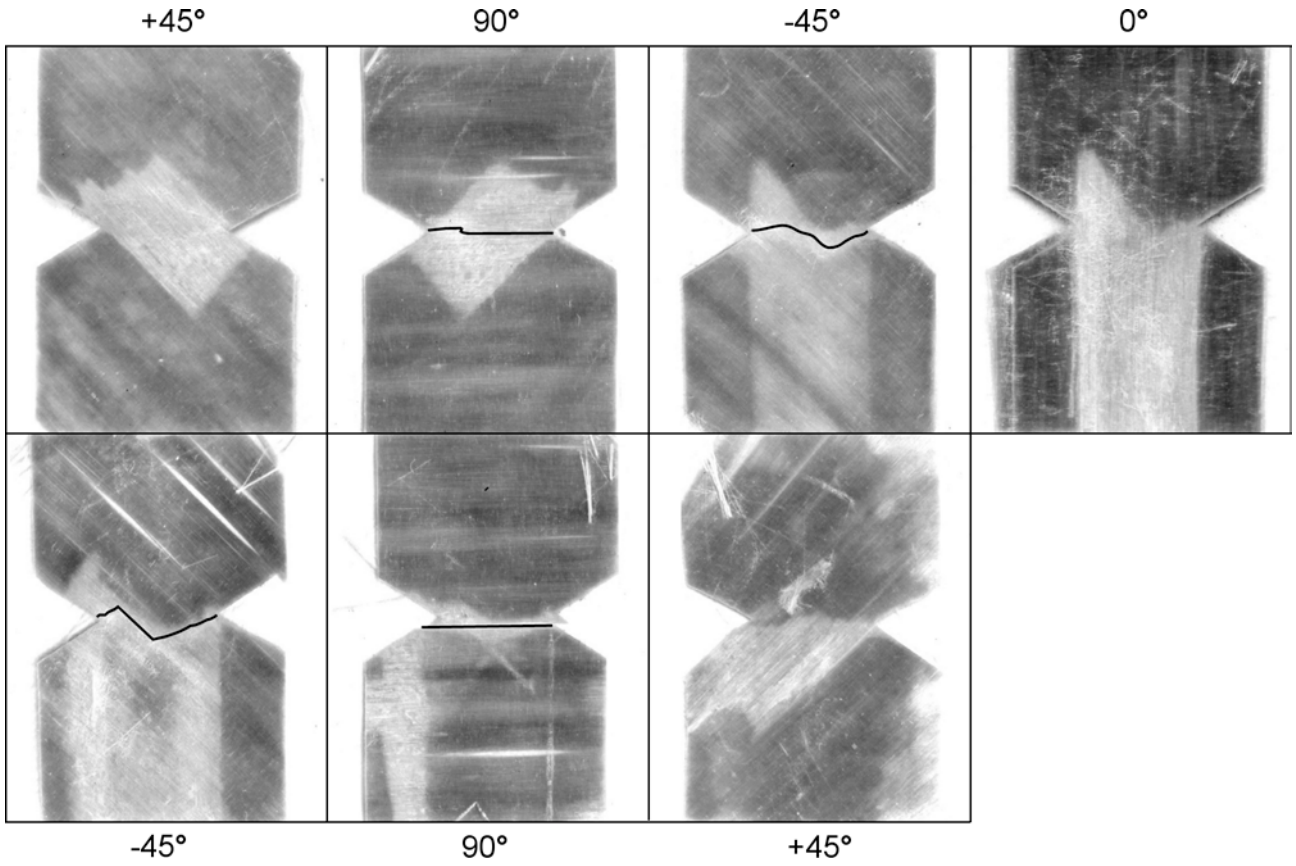

Figure 13 Deply of the $[+45/90/-45/0_2]_s$ specimen shown in Figure 11 showing delamination and fibre failure location

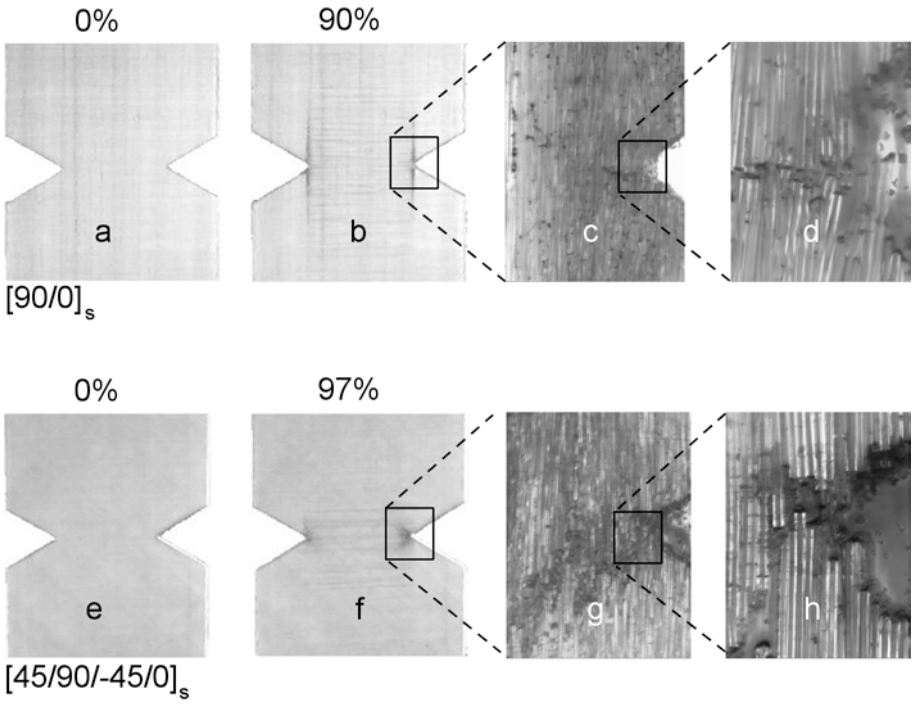

Figure 14 Damage patterns and microscope views of interrupted tests

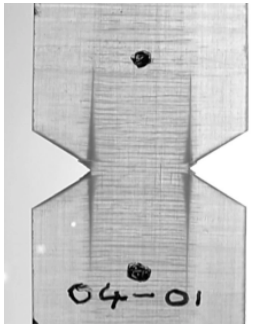

Figure 15 Matrix cracking in a 20mm wide cross-ply specimen

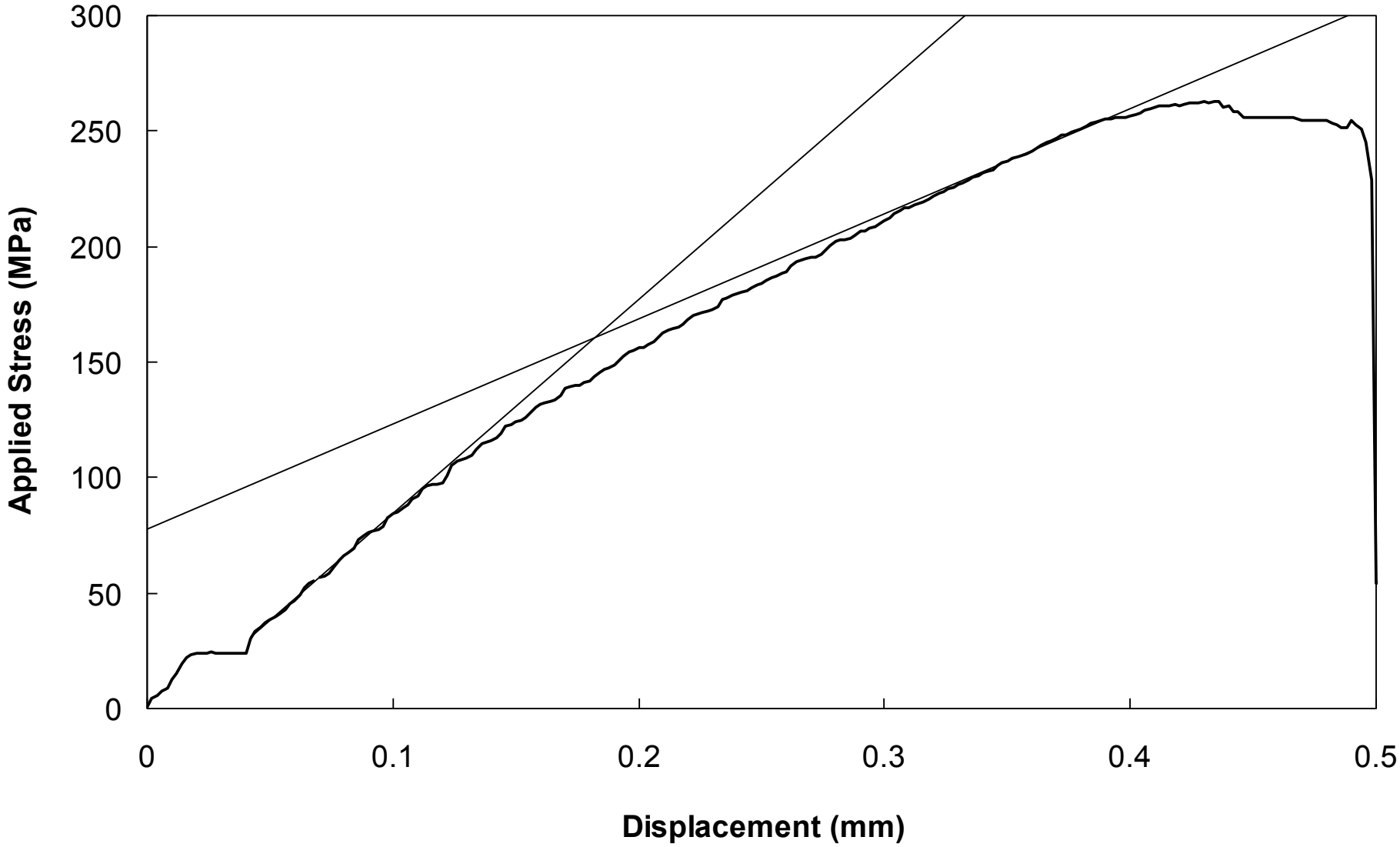

Figure 16 Applied stress-displacement curve for a 20mm wide $[90/0]_s$ specimen and stiffness reduction

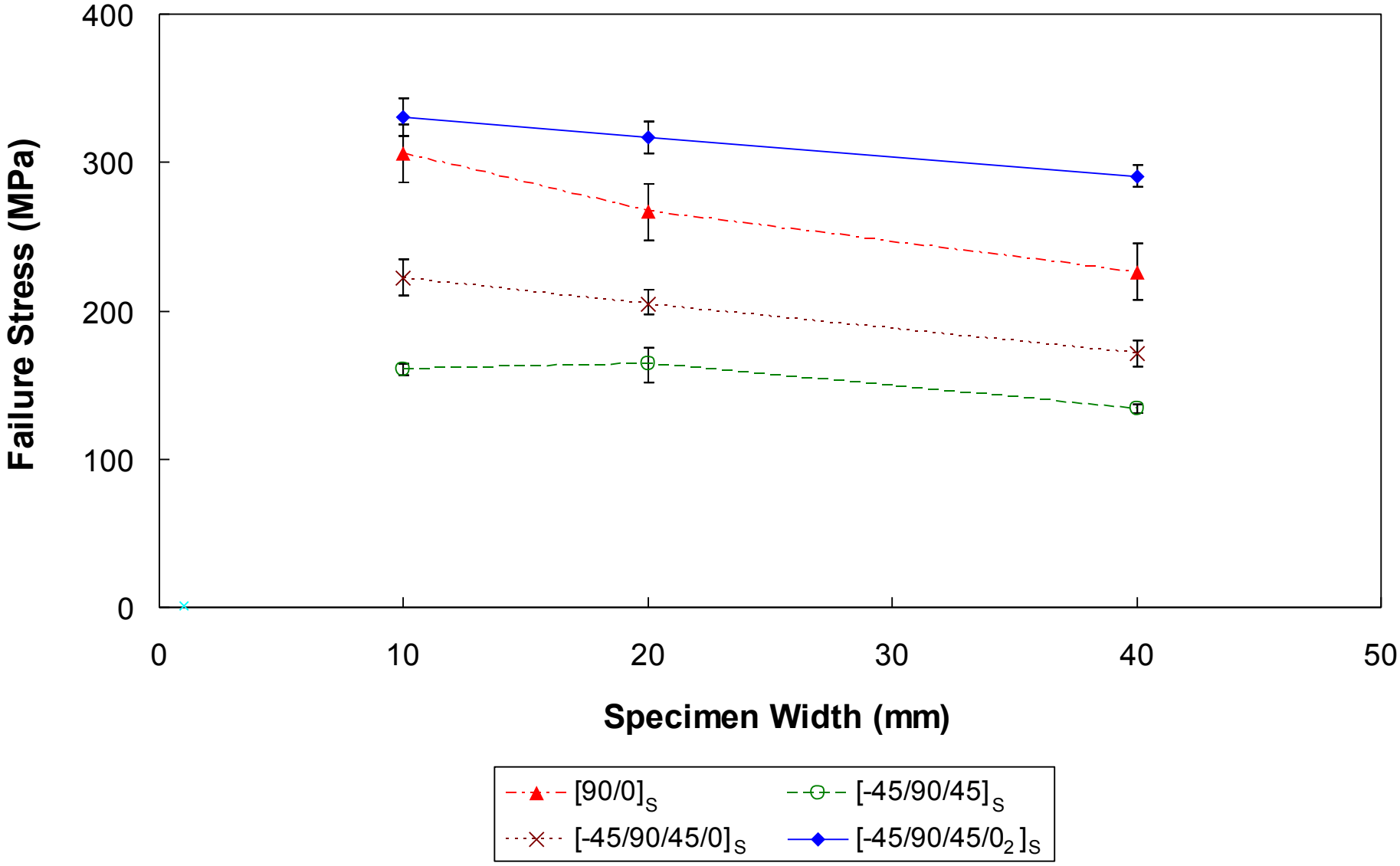

Figure 17 The effect of size on specimen strength for all layups tested

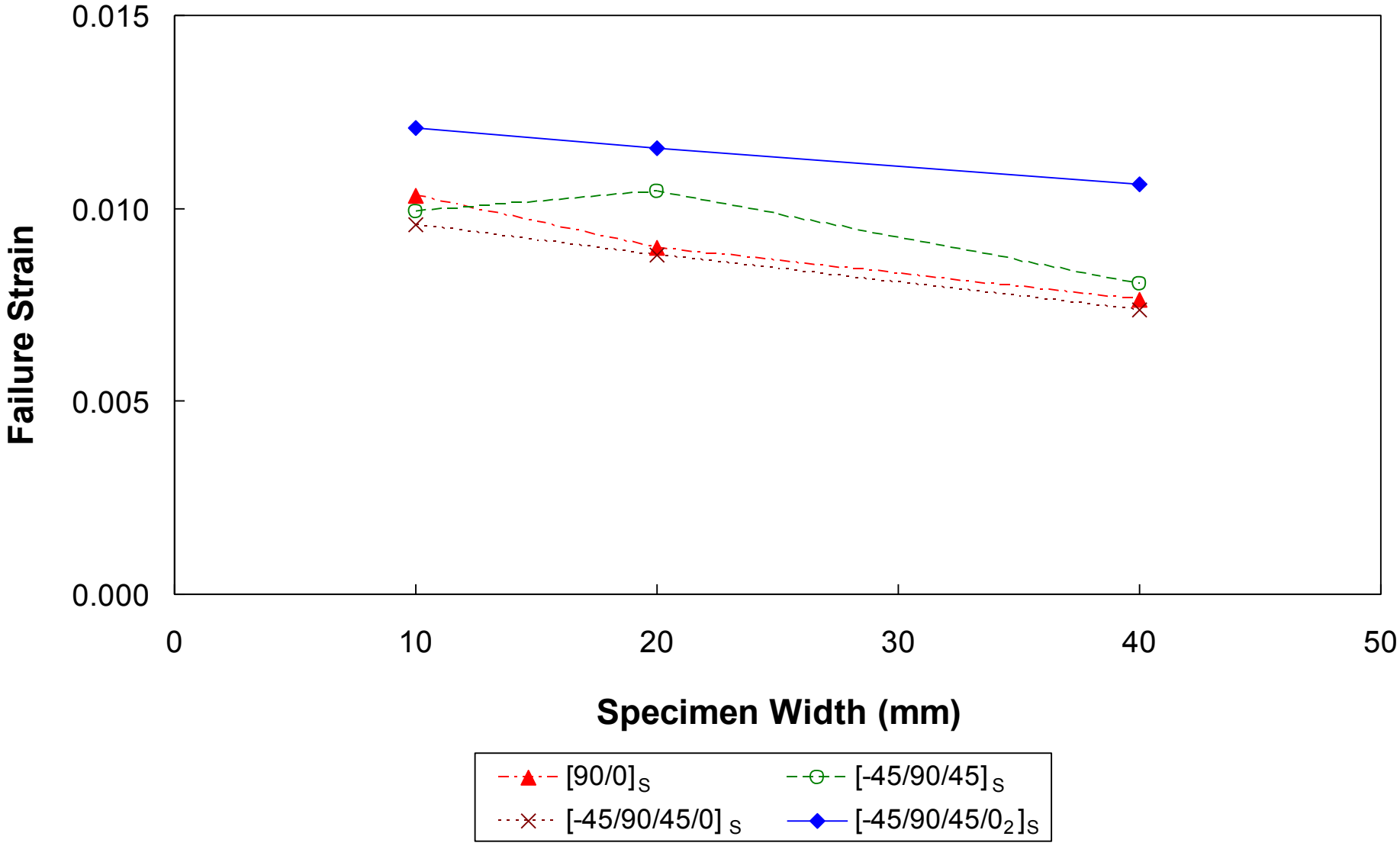

Figure 18 Failure strains calculated from far field applied stress and effective modulus

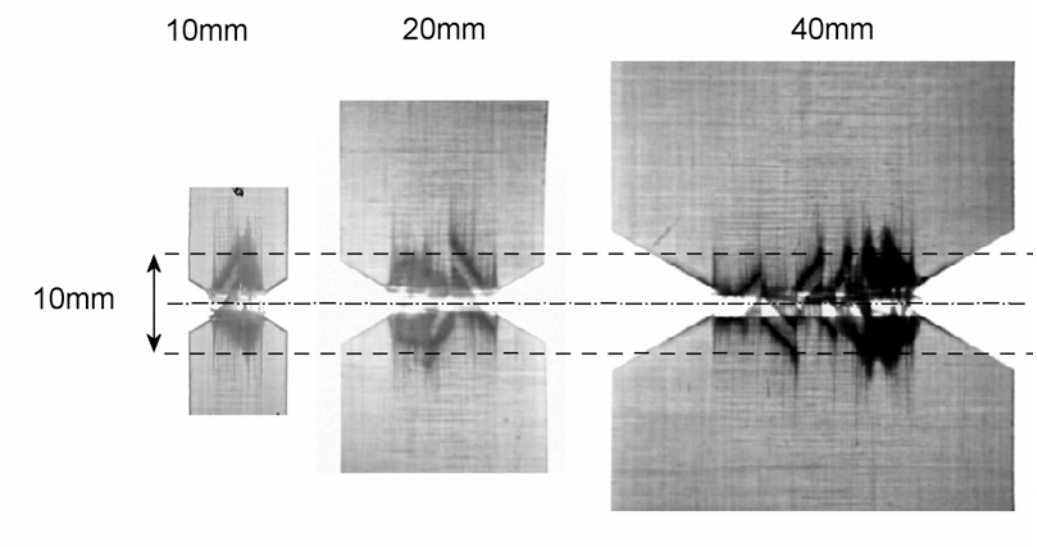

Figure 19 Damage zone size for typical cross-ply specimens

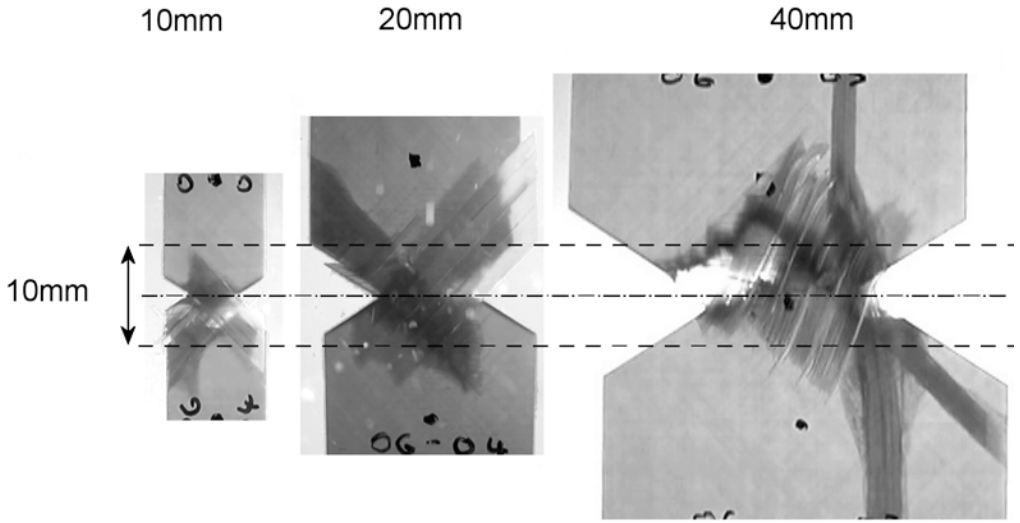

Figure 20 Damage zone size for typical quasi-isotropic specimens

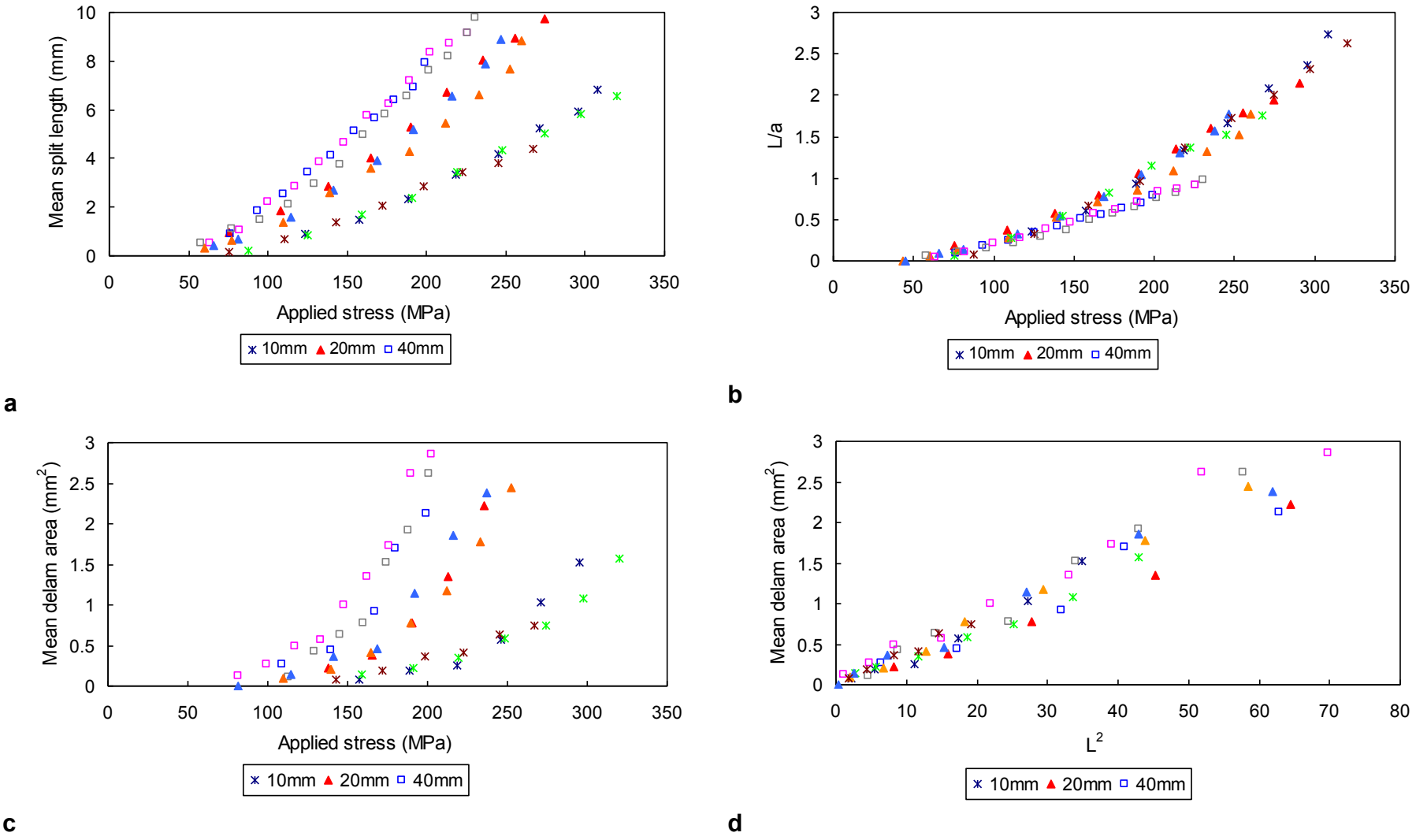

Figure 21a-d 0° split and delamination growth rate data for $[90/0]_s$ 10,20 and 40mm wide specimens

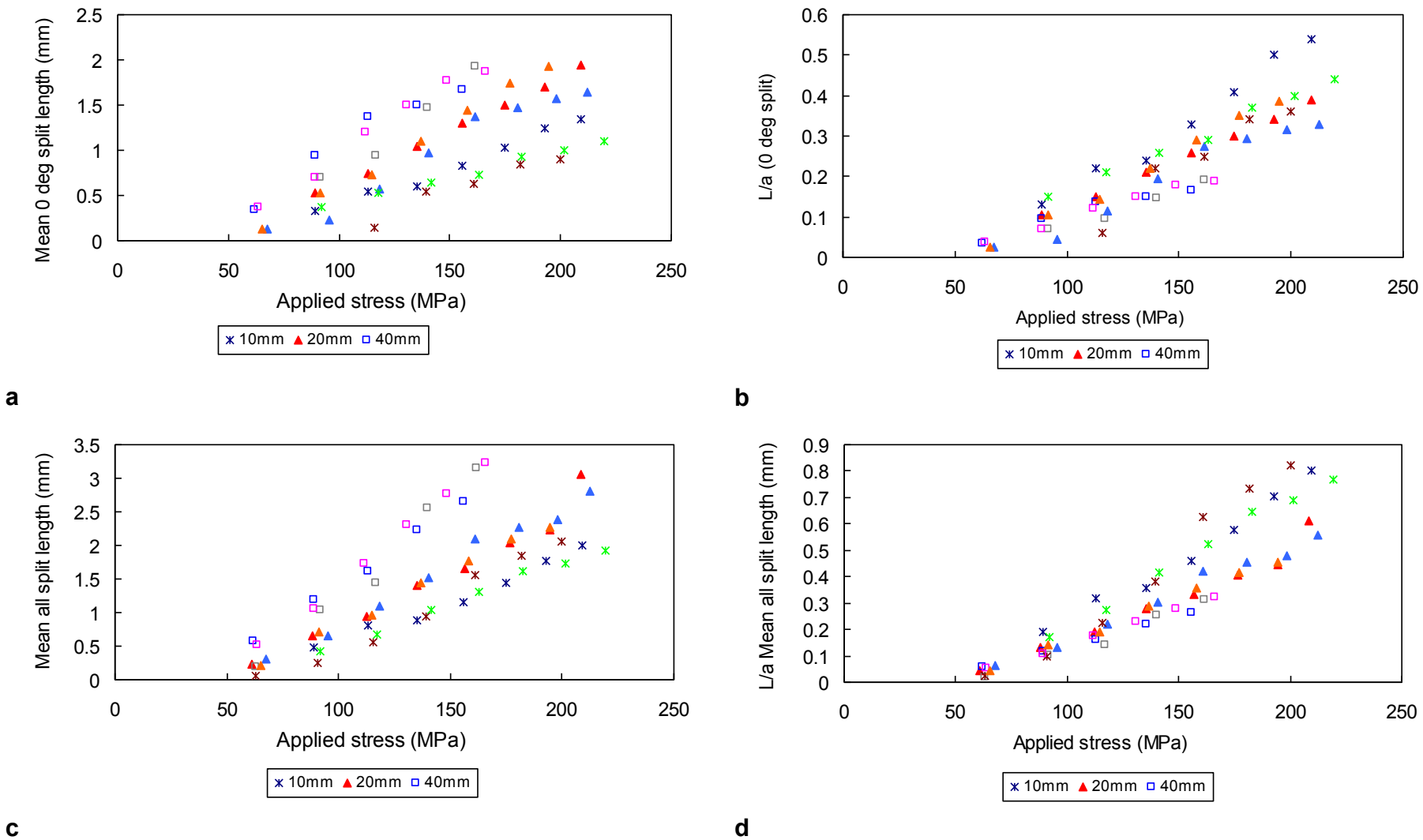

Figure 22a-d Split rate data for $[45/90/-45/0]_s$ 10,20 and 40mm wide specimens

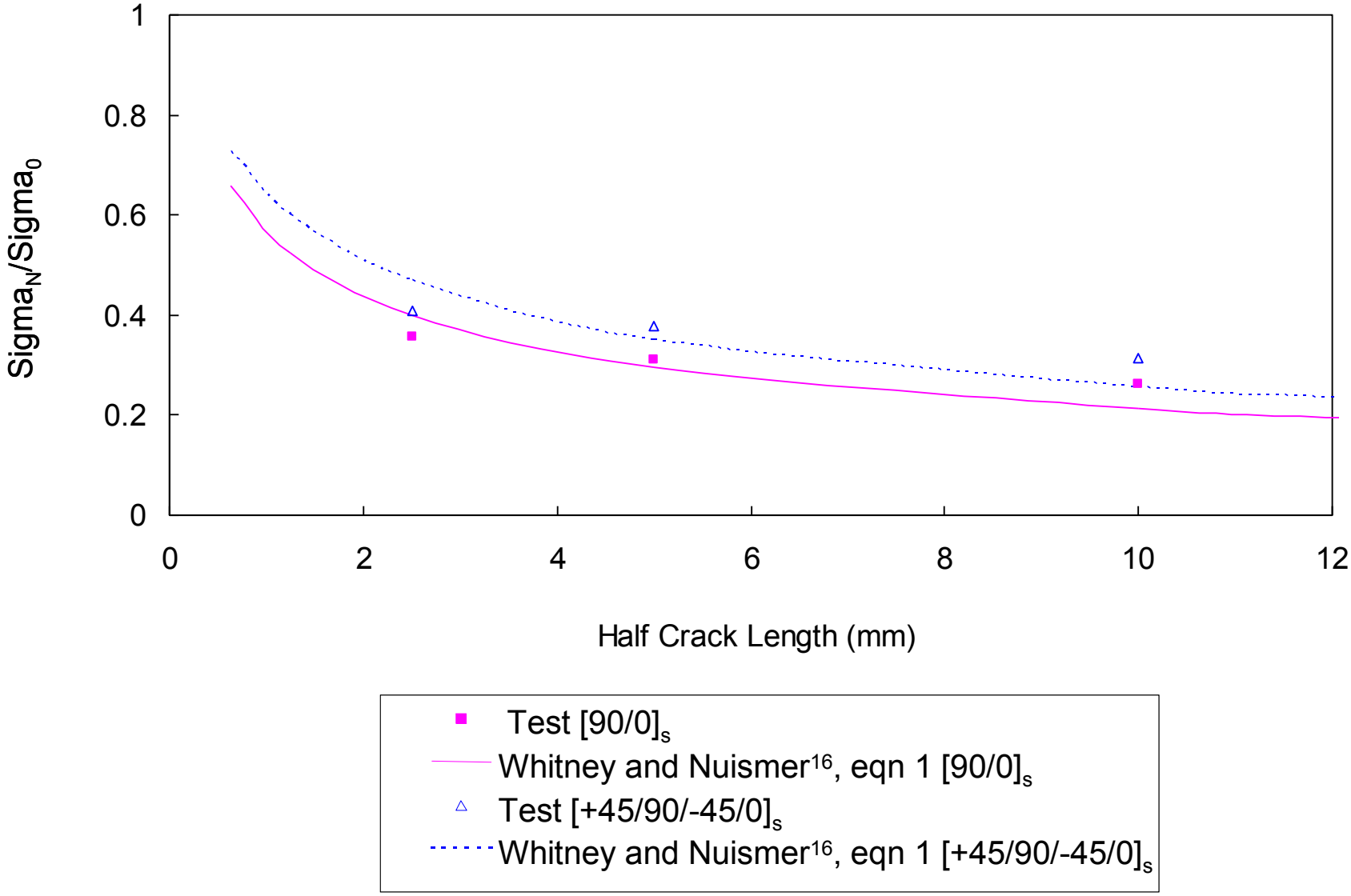

Figure 23 Average stress criterion[16] compared with test results

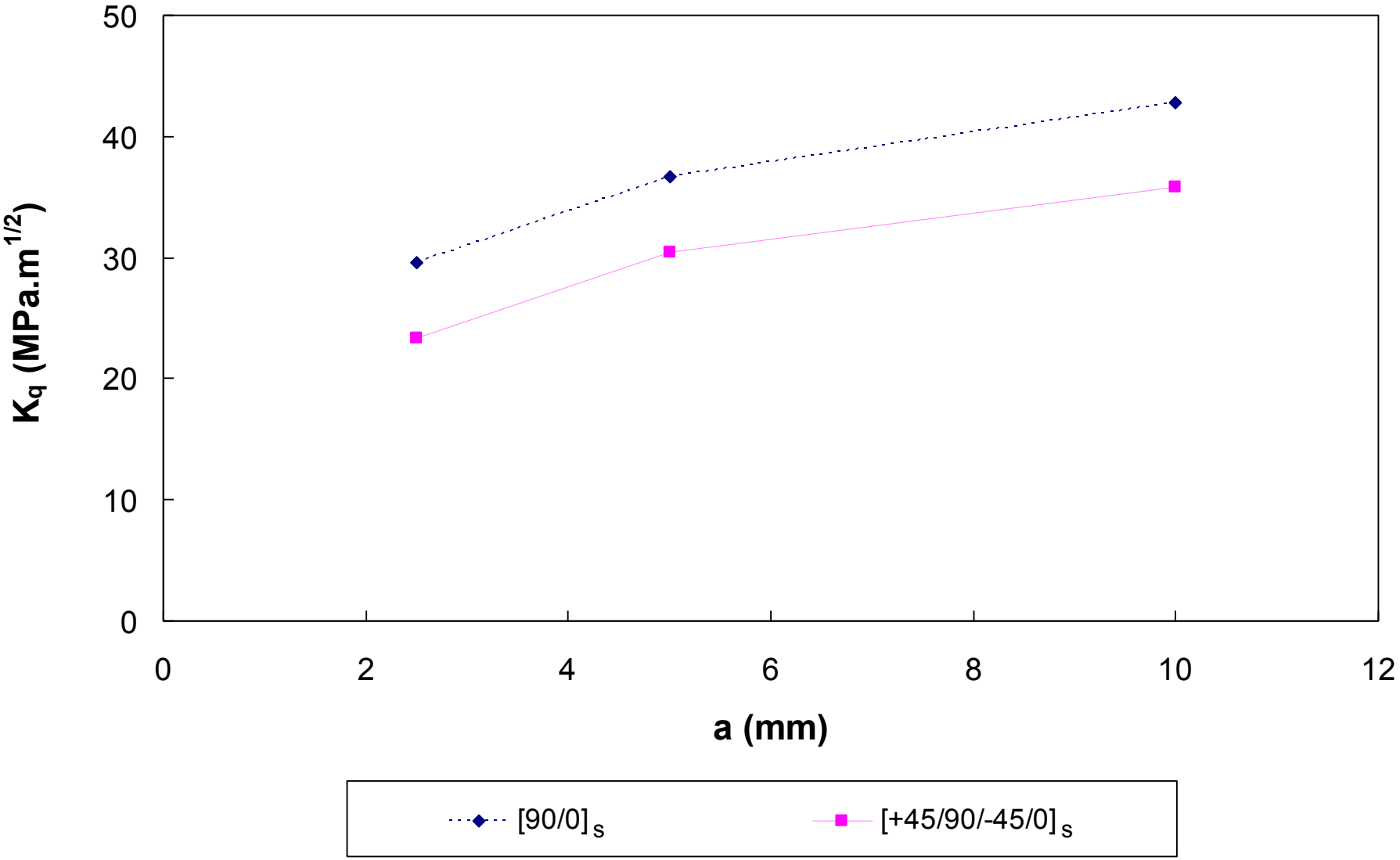

Figure 24 Calculated values for laminate fracture toughness